An Atomic Charge−Charge Flux−Dipole Flux Atom-in-Molecule Decomposition for Molecular Dipole-Moment Derivatives and Infrared Fundamental Intensities

Roberto L. A. Haiduke and Roy E. Bruns

Instituto de Química, Universidade Estadual de Campinas, CP 6154, 13083-970 Campinas, SP, Brazil

Received: October 11, 2004; In Final Form: January 14, 2005

The molecular dipole moment and its derivatives are determined from atomic charges, atomic dipoles, and their fluxes obtained from AIM formalism and calculated at the MP2(FC)/6-311++G(3d,3p) level for 16 molecules: 6 diatomic hydrides, CO, HCN, OCS, CO_2, CS_2, C_2H_2, C_2N_2, H_2O, H_2CO, and CH_4. Root-mean-square (rms) errors of 0.052 D and 0.019 e are found for the dipole moments and their derivatives calculated using AIM parameters when compared with those obtained directly from the MP2(FC)/6-311++G(3d,3p) calculations and 0.097 D and 0.049 e when compared to the experimental values. The major deviations occur for the NaH, HF, and H_2O molecules. Parallel polar tensor elements for the diatomic and linear polyatomic molecules, except H_2, HF, LiH, and NaH, have values resulting from cancellations of substantial contributions from atomic charge fluxes and atomic dipole fluxes. These fluxes have a large negative correlation coefficient, −0.97. IR fundamental intensity sums for CO, HCN, OCS, CO_2, CS_2, C_2H_2, C_2N_2, H_2CO, and CH_4 calculated using AIM charges, charge fluxes, and atomic dipole fluxes have rms errors of 14.9 km mol^{-1} when compared with sums calculated directly from the molecular wave function and 36.2 km mol^{-1} relative to experimental values. The classical model proposed here to calculate dipole-moment derivatives is compared with the charge−charge flux−overlap model long used by spectroscopists for interpreting IR vibrational intensities. The utility of the AIM atomic charges and dipoles was illustrated by calculating the forces exerted on molecules by a charged particle. AIM quantities were able to reproduce forces due to a +0.1 e particle over a 3−8-Å separation range for the CO and HF molecules in collinear and perpendicular arrangements. These results show that IR intensities do contain information relevant to the study of intermolecular interactions.

1. Introduction

The study of atomic properties such as net charges, dipoles, and fluxes during molecular vibrations has been an important research area in chemistry,[1−5] because it could provide a simple model for describing IR fundamental intensities using electronic structure factors. These intensities are proportional to the squares of the molecular dipole-moment derivatives with respect to their normal coordinates. A number of different models have been proposed for the explanation of molecular dipole-moment derivatives on the basis of partitioning into contributions from static charge, charge flux, overlap, atomic, and homopolar dipole flux terms.[6−8] These partition models have used Mulliken[9,10] or GAPT[11] charges as static charges, and charge-flux contributions are calculated by derivatives of the charges under atomic displacements.

A large variety of charge models have been developed over the years. One of these models for the calculation of atomic charges along with other atomic properties was proposed by Bader.[12,13] In this model, atoms in molecules (AIM) are defined by surfaces, called zero-flux surfaces. These surfaces are based on the characteristics of electronic density topology such as minima, maxima, or saddle points. These are important attributes for a charge model, because the electronic density can be experimentally measured via X-ray diffraction experiments. After the determination of the atomic boundaries in a molecule, the atomic charge of atom A is simply given by

$$q_A = Z_A - \int_A \rho(r)\, d\tau \qquad (1)$$

where Z_A is the nuclear charge and $\rho(r)$ is the electronic charge density. In this equation, the integration is carried out over the atomic basin.[12] However, the use of AIM charges alone is not enough to reproduce the molecular dipole moment.[14] This owes to asymmetries from spherical distributions of electronic charges around atoms in molecules. Hence, atomic dipoles are necessary for a more complete description of the molecular dipoles. These atomic dipoles are calculated from

$$m_A = -e \int_A r_A \rho(r)\, d\tau \qquad (2)$$

where the r_A vector, with origin at nucleus A, is averaged over the charge density of the atom.

If atomic charges and atomic dipoles are used, the Cartesian components of the molecular dipole moment can be represented by

$$\mu_x = \sum_A q_A x_A + \sum_A m_{A,x} \qquad (3)$$

where x represents a generic direction. Molecular dipole moments calculated from eq 3 using AIM charges and atomic dipoles obtained from molecular wave functions have been shown to be in almost exact agreement with those calculated directly from the same wave function.[15]

Their derivatives, based on eq 3, must include terms such as atomic charges, charge fluxes, and atomic dipole fluxes as already pointed out by Bader and co-workers.[14] This leads to a new dipole-moment derivative decomposition scheme involving only classically interpretable terms.[16]

10.1021/jp045357u CCC: $30.25

One can expect excellent agreement between dipole-moment derivatives calculated from these electronic structure parameters and those obtained directly from the molecular wave functions, because the only significant decomposition errors arise from numerical inaccuracies in defining the atomic boundaries within molecules.

Quantum chemical computational procedures have improved significantly in the past years. One can now expect that the calculation of AIM atomic charges and dipoles as well as their fluxes will result in IR intensities in good agreement with the experimental values. In this case, a quantitative understanding of gas-phase IR fundamental intensities based on chemical quantities (i.e., atomic charges, atomic charge fluxes, and atomic dipole fluxes) would be obtained. Here, we test the accuracy of this AIM atomic charge−charge flux−dipole flux (CCFDF) decomposition using MP2 perturbation theory with a 6-311++G-(3d,3p) basis function set for some diatomic molecules, most linear polyatomic molecules for which complete sets of gas-phase fundamental intensities have been measured, and the water, formaldehyde, and methane polyatomic molecules. Furthermore, the calculation of interaction forces between charged particles and molecules with electronic distributions represented by these AIM quantities is also shown and compared with those calculated directly from the molecular wave function. The results of these calculations are expected to provide evidence as to whether electronic structure parameters capable of describing IR intensities are also useful for studying intermolecular interactions.

2. Calculations

A 6-311++G(3d,3p) basis set was used in all calculations performed in this work by the *Gaussian 98*[17] program on a DEC ALPHA workstation. The DENSITY=CURRENT keyword was employed to obtain relaxed densities[18] corresponding to frozen-core MP2 perturbation energies. The molecular dipole moments and dipole-moment derivatives and the AIM atomic charges, atomic dipoles, charge fluxes, and atomic dipole fluxes were calculated from these relaxed MP2 densities.

The atomic charge flux and atomic dipole flux terms were calculated by means of numerical derivatives of AIM atomic charges and atomic dipoles in different nuclear arrangements around the equilibrium geometry. Atomic displacements of 0.01 Å were used to calculate these derivatives.

3. Results and Discussion

One tetrahedral, two planar, and a large number of linear molecules are analyzed here. Table 1 contains MP2(FC)/6-311++G(3d,3p) calculated AIM charges and dipoles for their atoms. These will be referred to as static atomic properties.

Considering that atomic dipoles are vectorial quantities, the molecular orientation adopted must be clearly shown. Hence, linear molecules were placed along the *z* axis. The hydrogen atom occupied the positive direction in the case of hydrides and HCN. O and S atoms were, respectively, in this position for CO and OCS. The orientations employed for the nonlinear systems are shown in Figure 1. The values given in Table 1 for atoms of linear molecules with a center of symmetry are those corresponding to atoms situated in the positive direction of the *z* axis.

For diatomic molecules, Table 1, atomic charges appear to be highly correlated with electronegativity. This can be easily seen by the hydrogen charge variation for diatomic systems where this atom is bonded to alkali metals and halogens. On the other hand, no obvious trend can be observed for the corresponding atomic dipole magnitudes. The direction of the hydrogen atomic dipole vector in the alkali metal compounds is pointed away from the metal atom, whereas in the halogen-containing molecules, these dipoles point toward the halogens. Of the diatomic molecules, CO has the highest atomic dipoles, 4.2 and 2.1 D for carbon and oxygen, respectively, owing to highly anisotropic electronic distributions.

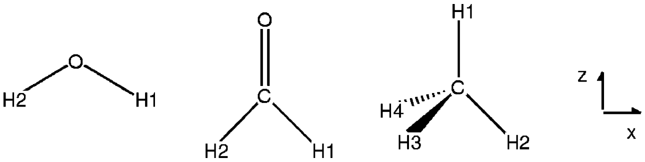

Figure 1. Molecular orientations for H_2O, H_2CO, and CH_4 molecules.

TABLE 1: AIM Charges and Atomic Dipoles Calculated with MP2(FC)/6-311++G(3d,3p)

molecule	A	q_A (e)	$m_{A,x}$ (D)	$m_{A,z}$ (D)
H_2	H	0.000		−0.255
HF	H	0.740		−0.182
	F	−0.740		−1.125
HCl	H	0.240		−0.301
	Cl	−0.240		−0.041
HBr	H	0.062		−0.185
	Br	−0.062		0.631
LiH	H	−0.909		1.013
	Li	0.909		−0.004
NaH	H	−0.800		0.361
	Na	0.800		0.064
CO	C	1.101		4.168
	O	−1.101		2.107
HCN	H	0.169		−0.242
	C	0.799		−2.235
	N	−0.968		−0.779
OCS	O	−1.018		−1.499
	C	0.524		−4.364
	S	0.494		−2.813
CO_2	C	2.137		0.000
	O	−1.068		1.536
CS_2	C	−1.096		0.000
	S	0.548		−3.006
HCCH	C	−0.121		−0.341
	H	0.121		−0.276
NCCN	C	0.836		1.609
	N	−0.836		0.614
H_2O	O	−1.159		0.789
	H1	0.580	−0.260	0.241
H_2CO	C	1.048		2.083
	O	−1.040		1.110
	H1	−0.004	−0.250	0.224
CH_4	C	0.086		0.000
	H1	−0.021		−0.353

These conclusions can be extended to the other molecules. Furthermore, atoms that participate in multiple bonds involving heteroatoms appear to have highly anisotropic environments. Atomic dipoles from 1.1 to 4.4 D are observed in double bonds between carbon and oxygen or sulfur. Triple bonds between carbon and nitrogen present a somewhat lower but significant range of dipole values between 0.6 and 2.2 D.

Figure 2 presents a graph of the absolute magnitudes of the molecular dipole moments calculated from eq 3 using AIM charges and atomic dipoles against those calculated directly from the MP2(FC)/6-311++G(3d,3p) approach as well as against the experimental values. The corresponding values are given in Table 2. The root-mean-square (rms) error of the AIM model values is 0.052 D when compared with values calculated from the molecular wave function. This is about 1% of the range in dipole-moment values that vary from 0.26 D to almost 7 D. The largest deviations are observed for HF (0.13 D) and H_2O

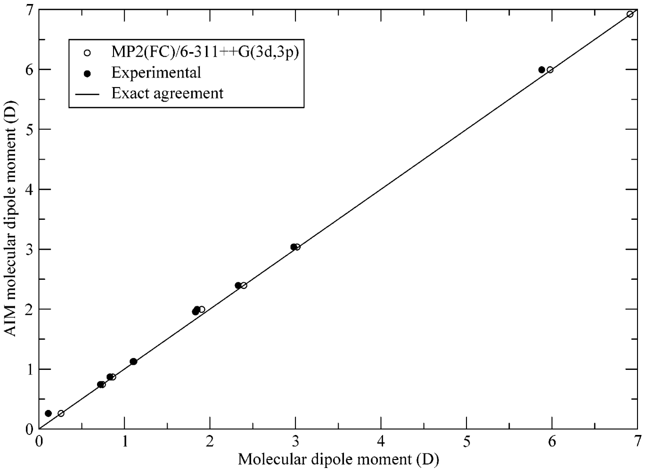

Figure 2. Comparison of experimental molecular dipole moments and those calculated directly at the MP2(FC)/6-311++G(3d,3p) level with those obtained from AIM atomic charges and atomic dipoles.

TABLE 2: Experimental and Calculated Molecular Dipole Moments[a]

molecule	$|p_z|$ exp (D)	p_z MP2 (D)	p_z AIM (D)
HF	1.83	1.83	1.96
HCl	1.11	1.10	1.13
HBr	0.83	0.86	0.87
LiH	5.88	−5.98	−5.99
NaH		−6.91	−6.92
CO	0.11	0.26	0.26
HCN	2.98	3.02	3.04
OCS	0.72	0.74	0.74
H_2O	1.85	−1.91	−2.00
H_2CO	2.33	−2.40	−2.40

[a] The calculated results were obtained directly from the MP2(FC)/6-311++G(3d,3p) approach and from aim atomic charges and atomic dipoles in the molecular orientations adopted here.

TABLE 3: AIM Charge Fluxes and Dipole Fluxes for Atoms in Diatomic Molecules along the *z* Cartesian Axis

molecule	A[a]	$\partial q_A/\partial z_B$ (e Å^{-1})[a]	$\partial m_{A,z}/\partial z_B$ (e)[a]	$\partial m_{A,x}/\partial x_B$ (e)[a]
H_2	H*	0.000	0.183	0.000
HF	H*	−0.470	−0.138	−0.041
	F	0.470	0.082	−0.255
HCl	H*	0.515	0.056	−0.049
	Cl	−0.515	−0.722	−0.007
HBr	H*	0.580	0.069	−0.027
	Br	−0.580	−0.820	0.093
LiH	H*	0.005	0.434	0.131
	Li	−0.005	0.005	0.000
NaH	H*	−0.070	0.405	0.039
	Na	0.070	−0.026	0.007
CO	C	−1.370	−0.630	0.762
	O*	1.370	−0.336	0.385

[a] Both B and * indexes refer to the atom placed in the positive *z* direction.

(0.09 D). The agreement of the AIM dipole-moment results with the experimental values[19] is about twice as large, 0.097 D, but still very good. The signs of the dipole moments calculated from AIM parameters and directly from the molecular wave function are in exact agreement. The atomic dipoles in CO are responsible for an inversion of the molecular dipole direction. Charges alone indicate that carbon is positive while oxygen is negative with a 6.01-D molecular dipole moment. Inclusion of the atomic dipole contribution changes this value to 0.26 D, in good agreement with the experimental value of 0.13 D.

Tables 3−8 present the charge and dipole fluxes for all atoms in the molecules analyzed. In the case of these dynamic properties, charge flux in diatomic molecules of Table 3 is always significant, except for H_2, LiH, and NaH molecules. Hydrogen atomic dipole fluxes for LiH and NaH, on the other hand, are larger for these molecules than for the hydrogen halides. The negatively charged electronic distribution around the hydrogen atom is polarized by the positively charged metal atom.

The dynamic properties, along with the static ones, can be useful to describe molecular dipole derivatives. These derivatives, according to eq 3, are given by

$$\frac{\partial p_x}{\partial x_A} = p_{xx}^{(A)} = q_A + \sum_i x_i \frac{\partial q_i}{\partial x_A} + \sum_i \frac{\partial m_{i,x}}{\partial x_A} \tag{4}$$

and

$$\frac{\partial p_y}{\partial x_A} = p_{yx}^{(A)} = \sum_i y_i \frac{\partial q_i}{\partial x_A} + \sum_i \frac{\partial m_{i,y}}{\partial x_A} \tag{5}$$

These equations show that dipole-moment derivatives are composed of three different contributions: (1) the static atomic charge, (2) a weighted charge flux, and (3) the atomic dipole flux. Any of these contributions can dominate, depending on the molecule and type of distortion under study.

In Tables 9 and 10, one can see the experimental[20−29] and calculated dipole-moment derivatives for the molecules studied here. Figure 3 shows a graph of the derivatives calculated from the AIM parameters against derivatives calculated directly from the molecular wave function, as well as derivatives obtained experimentally. The agreement between the values calculated directly from the MP2(FC)/6-311++G(3d,3p) approach and from AIM quantities, as prescribed by eqs 4 and 5, is very satisfactory. For the linear molecules, a very small 0.0065 e rms error is found for the dipole derivatives perpendicular to the bond, whereas a somewhat larger error of 0.0245 e occurs for the parallel derivatives. For the nonlinear molecules, the pooled rms error for $p_{xx}^{(A)}$, $p_{yy}^{(A)}$, and $p_{zz}^{(A)}$ is 0.020 e. The largest deviations, between 0.055 and 0.082 e, are observed for Cartesian derivatives of the HF, NaH, and H_2O molecules. The HF and H_2O molecules also presented the largest deviations in Table 2 between AIM and MP2 dipole-moment results, probably indicating that the source of error for these two molecules is caused by the numerical integration procedure of the AIM method. On the other hand, these dipole-moment results for NaH agree within 0.01 D, so the source of error, in this case, may be the size of the displacement used for the numerical estimates of the atomic charge and atomic dipole derivatives in eqs 4 and 5.

The derivatives obtained using AIM parameters and the CCFDF decomposition of eqs 4 and 5 are also in good agreement with the experimental derivatives of linear molecules. The rms errors are 0.026 and 0.082 e for perpendicular and parallel derivatives, respectively. For all the molecules of this study, the pooled rms error for the experimental and AIM results is 0.049 e. In addition to the error sources mentioned already, the discrepancies between the results using the AIM parameters and the experimental values can be caused by inaccuracies in the MP2(FC)/6-311++G(3d,3p) theoretical treatment as well as uncertainties in the experimental determinations.

Besides providing accurate theoretical results for dipole-moment derivatives, the AIM CCFDF decomposition permits an appealing classical description of electronic charge behavior during molecular vibrations. In Tables 11 and 12, charge, charge

TABLE 4: AIM Charge Fluxes and Dipole Fluxes for Atoms in Triatomic Linear Molecules along the *z* Cartesian Axis

		$\partial q_{A}/\partial z_{B}$ (e Å^{-1})[b]			$\partial m_{A,z}/\partial z_{B}$ (e)[b]			$\partial m_{A,x}/\partial x_{B}$ (e)[b]		
molecule	A[a]	*i*	*j*	*k*	*i*	*j*	*k*	*i*	*j*	*k*
HCN	H*	0.795	−0.760	−0.035	0.034	−0.053	0.013	−0.048	0.049	−0.001
	C	−0.715	−2.270	2.985	−0.833	1.934	−1.101	0.167	−0.718	0.551
	N	−0.075	3.025	−2.950	−0.040	1.249	−1.209	−0.030	−0.081	0.112
OCS	O	−1.445	1.260	0.165	−0.569	0.746	−0.180	0.344	−0.402	0.058
	C	2.065	−3.980	1.920	−0.688	−0.045	0.733	0.584	−0.439	−0.145
	S*	−0.620	2.725	−2.105	−0.016	−1.529	1.545	−0.009	0.382	−0.380
CO_2	C	0.000		−1.915	1.487		−0.744	−0.779		0.389
	O	1.200		0.360	0.744		−0.159	−0.447		0.087
	O*	−1.200		1.555	0.744		−0.587	−0.447		0.360
CS_2	C	0.000		1.915	−1.831		0.916	0.110		−0.055
	S	−2.730		0.410	−1.558		−0.085	0.376		0.012
	S*	2.730		−2.325	−1.558		1.640	0.376		−0.388

[a] * index refers to the atom placed in the positive *z* direction. [b] The *i*, *j*, and *k* indexes refer respectively to B atoms as being the first, second, and third atom appearing in the second column for each molecule.

TABLE 5: AIM Charge Fluxes and Dipole Fluxes for Atoms in Tetratomic Linear Molecules along the *z* Cartesian Axis

		$\partial q_{A}/\partial z_{B}$ (e Å^{-1})[b]		$\partial m_{A,z}/\partial z_{B}$ (e)[b]		$\partial m_{A,x}/\partial x_{B}$ (e)[b]	
molecule	A[a]	*i*	*k*	*i*	*k*	*i*	*k*
HCCH	C*	0.590	−0.765	1.117	−0.852	−0.671	0.267
	C	−0.115	−0.055	−0.254	−0.008	0.532	−0.128
	H*	−0.645	0.815	−0.048	0.037	0.061	−0.055
	H	0.170	0.000	0.008	0.000	−0.013	0.006
NCCN	C*	3.025	−2.970	1.413	−1.175	−0.690	0.494
	C	0.040	0.010	−0.206	−0.026	0.213	−0.018
	N*	−3.010	2.960	1.302	−1.244	−0.076	0.093
	N	−0.050	0.000	−0.069	0.011	−0.023	0.005

[a] * index refers to the atom placed in the positive *z* direction. [b] The *i* and *k* indexes refer respectively to B atoms as being the first and third atom appearing in the second column for each molecule.

flux, and dipole flux contributions calculated at the MP2/6-311++G(3d,3p) level are given for dipole-moment derivatives relative to atomic Cartesian displacement coordinates (i.e., the polar tensor elements).

The hydrogen halides have small total derivatives that result from partial cancellations of the individual contributions. For HF, the negative charge flux contribution of the bond-stretching mode is partially canceled by the positive static charge contribution as shown in Figure 4. As the HF bond length increases, the positively charged hydrogen atom, $+0.74$ e, becomes more negatively charged, indicated by the δ^- symbol in the figure, at the expense of the electron density in the vicinity of the fluorine atom. In contrast to HF, hydrogen atoms in HCl and HBr have small static-charge contributions and large negative parallel dipole flux contributions, indicated by the (+ −) signs in the ellipses in Figure 4. These almost completely cancel the positive charge flux contributions, resulting in quite small dipole-moment derivatives.

The metal hydrides have very negatively charged hydrogen atoms and very small charge flux contributions consistent with their ionic natures. However, the total dipole-moment derivatives of LiH and NaH are about one-half of that expected for an ionic diatomic species, owing to a partial cancellation of the static-charge contribution by a substantial positive dipole flux contribution. As can be seen in Table 3, only the atomic dipoles of the negatively charged hydrogen atoms in these molecules provide significant flux values.

The stretching mode of the CO molecule has reinforcing charge and dipole flux contributions that are partially canceled by a large charge flux. This cancellation of the flux contributions

TABLE 6: AIM Charge Fluxes and Dipole Fluxes for Atoms in the Water Molecule

	$\partial q_{A}/\partial x_{B}$ (e Å^{-1})[a]		$\partial q_{A}/\partial z_{B}$ (e Å^{-1})[a]		$\partial m_{A,x}/\partial x_{B}$ (e)[a]		$\partial m_{A,y}/\partial y_{B}$ (e)[a]		$\partial m_{A,z}/\partial z_{B}$ (e)[a]		$\partial m_{A,z}/\partial x_{B}$ (e)[a]		$\partial m_{A,x}/\delta z_{B}$ (e)[a]	
A	*i*	*j*	*i*	*j*	*i*	*j*	*i*	*j*	*i*	*j*	*i*	*j*	*i*	*j*
O	0.000	0.445	1.210	−0.605	−0.196	0.098	0.280	−0.140	−0.061	0.029	0.000	−0.164	0.000	−0.184
H1	0.535	−0.490	−0.605	0.510	0.037	−0.032	0.086	−0.078	0.095	−0.085	−0.005	0.003	−0.013	−0.013
H2	−0.535	0.050	−0.605	0.095	0.037	−0.005	0.086	−0.007	0.095	−0.011	0.005	0.000	0.013	−0.026

[a] The *i* and *j* indexes refer respectively to B atoms as being the first and second atom appearing in the first column.

TABLE 7: AIM Charge Fluxes and Dipole Fluxes for Atoms in the H_2CO Molecule

	$\partial q_{A}/\partial x_{B}$ (e Å^{-1})[a]			$\partial q_{A}/\partial z_{B}$ (e Å^{-1})[a]			$\partial m_{A,x}/\partial x_{B}$ (e)[a]			$\partial m_{A,y}/\partial y_{B}$ (e)[a]		
A	*i*	*j*	*k*	*i*	*j*	*k*	*i*	*j*	*k*	*i*	*j*	*k*
C	0.000	0.000	−0.520	1.870	−2.205	0.170	0.482	0.333	−0.407	−0.591	0.433	0.079
O	0.000	0.000	−0.020	−1.485	1.520	−0.020	−0.460	0.344	0.058	−0.309	0.229	0.040
H1	−0.125	−0.075	0.370	−0.195	0.340	−0.185	−0.042	0.032	0.021	−0.008	0.029	−0.038
H2	0.125	0.075	0.165	−0.195	0.340	0.040	−0.042	0.032	−0.013	−0.008	0.029	0.017

	$\partial m_{A,z}/\partial z_{B}$ (e)[a]			$\partial m_{A,z}/\partial x_{B}$ (e)[a]			$\partial m_{A,x}/\partial z_{B}$ (e)[a]		
A	*i*	*j*	*k*	*i*	*j*	*k*	*i*	*j*	*k*
C	0.847	−0.601	−0.124	0.000	0.000	0.397	0.000	0.000	0.235
O	0.654	−0.497	−0.079	0.000	0.000	0.042	0.000	0.000	0.064
H1	−0.034	−0.042	0.053	−0.122	0.082	0.034	−0.071	0.026	0.016
H2	−0.034	−0.042	0.024	0.122	−0.082	−0.003	0.071	−0.026	−0.032

[a] The *i*, *j*, and *k* indexes refer respectively to B atoms as being the first, second, and third atom appearing in the first column.

TABLE 8: AIM Charge Fluxes and Dipole Fluxes for Atoms in the Methane Molecule

	$\partial q_A/\partial x_B$ (e Å^{-1})[a]		$\partial q_A/\partial y_B$ (e Å^{-1})[a]		$\partial q_A/\partial z_B$ (e Å^{-1})[a]		$\partial m_{A,x}/\partial x_B$ (e)[a]		$\partial m_{A,y}/\partial y_B$ (e)[a]		$\partial m_{A,z}/\partial z_B$ (e)[a]	
A	*i*	*j*	*i*	*j*	*i*	*j*	*i*	*j*	*i*	*j*	*i*	*j*
C	0.000	0.000	0.000	0.000	0.000	−0.620	0.484	0.143	0.482	0.144	0.482	−0.651
H1	0.000	0.000	0.000	0.000	−0.335	0.520	−0.038	0.016	−0.038	0.016	0.008	0.037
H2	−0.320	−0.055	0.000	0.000	0.110	0.030	0.003	0.003	−0.038	−0.002	−0.032	0.000
H3	0.160	0.030	−0.275	−0.050	0.110	0.030	−0.029	−0.003	−0.005	0.003	−0.032	0.000
H4	0.160	0.030	0.275	0.050	0.110	0.030	−0.029	−0.003	−0.005	0.003	−0.032	0.000

	$\partial m_{A,y}/\partial x_B$ (e)[a]		$\partial m_{A,z}/\partial x_B$ (e)[a]		$\partial m_{A,x}/\partial y_B$ (e)[a]		$\partial m_{A,z}/\partial y_B$ (e)[a]		$\partial m_{A,x}/\partial z_B$ (e)[a]		$\partial m_{A,y}/\partial z_B$ (e)[a]	
A	*i*	*j*	*i*	*j*	*i*	*j*	*i*	*j*	*i*	*j*	*i*	*j*
C	0.000	0.000	0.000	0.000	0.000	0.000	0.000	0.000	0.000	0.000	0.000	0.000
H1	0.000	0.000	0.000	0.000	0.000	0.000	0.000	0.000	0.000	0.000	0.000	0.000
H2	0.000	0.000	−0.016	0.058	0.000	0.000	0.000	0.000	−0.016	0.000	0.000	0.000
H3	−0.018	−0.003	0.008	−0.029	−0.018	−0.003	−0.013	0.051	0.008	0.000	−0.013	0.000
H4	0.018	0.003	0.008	−0.029	0.018	0.003	0.013	−0.051	0.008	0.000	0.013	0.000

[a] The *i* and *j* indexes refer respectively to B atoms as being the first and second atom appearing in the first column.

TABLE 9: Experimental and Calculated Cartesian Dipole-Moment Derivatives for Linear Molecules[a]

molecule	atom[b]	$p_{xx}^{(A)}$ (e)[c]			$p_{zz}^{(A)}$ (e)		
		exp	MP2	AIM	exp	MP2	AIM
HF	H	0.415	0.416	0.444	0.317	0.335	0.253
HCl	H	0.179	0.180	0.184	0.193	0.224	0.228
HBr	H	0.121	0.127	0.127	0.100	0.117	0.130
LiH	H	−0.747	−0.776	−0.778	−0.473	−0.462	−0.462
NaH	H		−0.753	−0.754		−0.558	−0.503
CO	O	0.022	0.047	0.048	−0.729	−0.503	−0.509
HCN	H	0.237	0.256	0.257	0.218	0.253	0.264
	C	0.084	0.050	0.049	−0.292	−0.392	−0.411
	N	−0.321	−0.306	−0.306	0.074	0.139	0.141
OCS	O	−0.103	−0.097	−0.099	−1.536	−1.572	−1.573
	C	0.101	0.070	0.065	2.345	2.481	2.487
	S	0.002	0.027	0.026	−0.809	−0.909	−0.894
CO_2	C	0.472	0.465	0.465	2.274	2.295	2.305
	O	−0.236	−0.232	−0.232	−1.137	−1.147	−1.161
CS_2	C	−0.168	−0.235	−0.234	2.400	2.473	2.477
	S	0.084	0.117	0.117	−1.200	−1.236	−1.250
HCCH	C	−0.226	−0.209	−0.210	−0.188	−0.209	−0.229
	H	0.226	0.209	0.210	0.188	0.209	0.226
NCCN	C	0.245	0.261	0.261	−0.123	−0.194	−0.187
	N	−0.245	−0.261	−0.262	0.123	0.194	0.197
rms	AIM/MP2			0.0065			0.0245
rms	AIM/exp			0.0261			0.0817

[a] Dipole-moment derivatives were calculated directly from the MP2(FC)/6-311++G(3d,3p) approach and from AIM quantities in the molecular orientations adopted here. [b] Results for atoms not listed in the table can be found using symmetry considerations. [c] $p_{xx}^{(A)} = p_{yy}^{(A)}$.

is very efficient, as is the one for the charge and dipole contributions to the CO static molecular moment.

The C−H stretching coordinate of HCN approximates the ν_1-band normal coordinate. Its dipole-moment derivative contributions for hydrogen atom displacement parallel to the molecular axis resemble those of HCl and HBr with large charge flux and dipole flux values that almost cancel one another. The CN stretching coordinate approximates the ν_3-normal coordinate. Displacement of the nitrogen atom in the positive direction along the molecular axis provokes large negative static charge and dipole flux terms and an even larger positive charge flux contribution. The charge flux contribution barely predominates, predicting identical signs for $\partial p_z/\partial z_H$ and $\partial p_z/\partial z_N$ as has been observed from experimental intensity results.[26] The values of $\partial p_z/\partial z_H$ and $\partial p_z/\partial z_N$ in HCN, +0.264 and +0.141 e, are very similar to the ones in C_2H_2, +0.227 e, and C_2N_2, +0.197 e. Furthermore, individual charge, charge flux, and dipole flux contributions for hydrogen and nitrogen appear to be transferable from HCN to C_2H_2 and C_2N_2.

Displacement of the carbon atom along the HCN molecular axis results in large charge flux and dipole flux contributions of opposite sign. For example, a relatively small $\partial p_z/\partial z_C$ polar tensor element of −0.411 e results from the cancellation of much larger charge (0.799 e), charge flux (−4.340 e), and dipole flux (3.130 e) contributions for HCN. Cancellation of these three effects also results in small $\partial p_z/\partial z_C$ polar tensor elements for C_2H_2 (−0.230 e) and C_2N_2 (−0.187 e).

The $\partial p_z/\partial z_O$ CO_2 tensor element consists of large negative charge and dipole flux contributions that are partially canceled by a positive charge flux contribution. The charge and dipole flux contributions to $\partial p_z/\partial z_O$ in OCS are very similar to those in CO_2 and have the same signs. However, the positive charge flux contribution in OCS is about one-half of the one found in CO_2.

The $\partial p_z/\partial z_S$ CS_2 and OCS polar tensor elements have positive static charge and dipole flux contributions, whereas the charge flux values are negative. Although the sulfur tensor contributions, especially the charge flux one, are hardly transferable for these molecules, it is interesting that the carbon charge, charge flux, and dipole flux contributions for OCS (+0.524, +2.791, and −0.828 e, respectively) are very similar to the averages of these contributions for CO_2 and CS_2 (0.521, 2.858, and −0.987 e, respectively).

The $\partial p_x/\partial x_A$ elements, corresponding to the rotational movements of the diatomic and linear polyatomic molecules, are easier to interpret than the $\partial p_z/\partial z_A$ elements. First, all charge flux contributions are zero by symmetry. Second, the charge contributions are the same as those for the displacements parallel to the molecular axis. Third, the dipole flux contributions can be classified into two groups: for atoms only participating in single bonds, the dipole flux contribution ranges from 0.0 to 0.3 e, and for atoms participating in double or triple bonds, they range from 0.4 to 1.7 e in absolute values. The only exception is the carbon atom of acetylene that has a dipole flux contribution equal, but of opposite sign, to the relatively small hydrogen contribution.

The analysis of polar tensor element contributions for nonlinear molecules is most conveniently carried out using the tensor invariants, $\bar{p}_A$, atomic mean dipole-moment derivatives and atomic anisotropies, β_A^2, because the individual tensor elements change depending on the molecular orientation used in the Cartesian coordinate space.[16] However, some general deductions can be made about charge and flux contributions to the water, formaldehyde, and methane polar tensor elements.

The water molecule has large charge and charge flux contributions that partially cancel for the in-plane polar tensor

TABLE 10: Experimental and Calculated Cartesian Dipole-Moment Derivatives for H_2O, H_2CO, and CH_4 Molecules[a]

		$p_{xx}^{(A)}$ (e)			$p_{yy}^{(A)}$ (e)			$p_{zz}^{(A)}$ (e)		
molecule	atom[b]	exp	MP2	AIM	exp	MP2	AIM	exp	MP2	AIM
H_2O	O	−0.460	−0.526	−0.469	−0.658	−0.676	−0.708	−0.298	−0.347	−0.319
	H1	0.230	0.263	0.231	0.329	0.338	0.355	0.149	0.174	0.159

		$p_{xz}^{(A)}$ (e)			$p_{zx}^{(A)}$ (e)		
		exp	MP2	AIM	exp	MP2	AIM
	H1	0.077	0.058	0.091	0.062	0.066	0.097

		$p_{xx}^{(A)}$ (e)			$p_{yy}^{(A)}$ (e)			$p_{zz}^{(A)}$ (e)		
molecule	atom	exp	MP2	AIM	exp	MP2	AIM	exp	MP2	AIM
H_2CO	C	0.728	0.758	0.750	0.118	0.131	0.131	0.933	0.899	0.906
	O	−0.424	−0.438	−0.439	−0.313	−0.321	−0.321	−0.803	−0.762	−0.774
	H1	−0.152	−0.160	−0.153	0.097	0.095	0.094	−0.065	−0.069	−0.071

		$p_{xz}^{(A)}$ (e)			$p_{zx}^{(A)}$ (e)		
		exp	MP2	AIM	exp	MP2	AIM
	H1	0.083	0.082	0.073	0.142	0.144	0.137

		$p_{xx}^{(A)}$ (e)			$p_{yy}^{(A)}$ (e)			$p_{zz}^{(A)}$ (e)		
molecule	atom	exp	MP2	AIM	exp	MP2	AIM	exp	MP2	AIM
CH_4	C	0.016	0.002	−0.016	0.016	0.002	−0.008	0.016	0.002	−0.003
	H1	0.062	0.060	0.047	0.062	0.060	0.053	−0.136	−0.122	−0.104
rms	AIM/MP2		0.0259			0.0166			0.0149	
rms	AIM/exp		0.0122			0.0244			0.0225	

[a] Dipole-moment derivatives were calculated directly from the MP2(FC)/6-311++G(3d,3p) approach and from AIM quantities in the molecular orientations adopted here. [b] Results for atoms not listed in the table can be found using symmetry considerations.

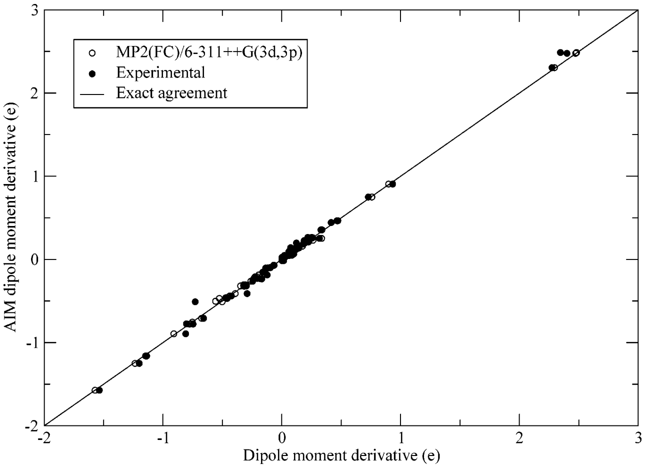

Figure 3. Comparison of experimental molecular dipole-moment derivatives and those calculated directly at the MP2(FC)/6-311++G-(3d,3p) level with those obtained from AIM atomic charges and fluxes.

TABLE 11: AIM Charge (C), Charge Flux (CF), and Dipole Flux (DF) Contributions to Polar Tensor Elements of the Linear Molecules Calculated at the MP2/6-311++G(3d,3p) Level (units of electrons, e)

		$p_{xx}^{(A)}$			$p_{zz}^{(A)}$			
molecule	atom	C	DF	total	C	CF	DF	total
H_2	H	0.000	0.000	0.000	0.000	0.000	0.000	0.000
HF	H	0.740	−0.296	0.444	0.740	−0.431	−0.056	0.253
	F	−0.740	0.296	−0.444	−0.740	0.431	0.056	−0.253
HCl	H	0.240	−0.056	0.184	0.240	0.655	−0.667	0.228
	Cl	−0.240	0.056	−0.184	−0.240	−0.655	0.667	−0.228
HBr	H	0.062	0.066	0.128	0.062	0.819	−0.751	0.130
	Br	−0.062	−0.066	−0.128	−0.062	−0.819	0.751	−0.130
LiH	H	−0.909	0.131	−0.778	−0.909	0.008	0.439	−0.462
	Li	0.909	−0.131	0.778	0.909	−0.008	−0.439	0.462
NaH	H	−0.800	0.046	−0.754	−0.800	−0.134	0.431	−0.503
	Na	0.800	−0.046	0.754	0.800	0.134	−0.431	0.503
CO	C	1.001	−1.148	−0.047	1.101	−1.558	0.966	0.509
	O	−1.001	1.148	0.047	−1.101	1.558	−0.966	−0.509
HCN	H	0.169	0.088	0.257	0.169	0.934	−0.839	0.264
	C	0.799	−0.750	0.049	0.799	−4.340	3.130	−0.411
	N	−0.968	0.662	−0.306	−0.968	3.406	−2.297	0.141
OCS	O	−1.018	0.919	−0.099	−1.018	0.718	−1.273	−1.573
	C	0.524	−0.459	0.064	0.524	2.791	−0.828	2.487
	S	0.494	−0.468	0.026	0.494	−3.486	2.098	−0.894
CO_2	C	2.137	−1.672	0.465	2.137	−2.806	2.974	2.305
	O	−1.068	0.836	−0.232	−1.068	1.397	−1.490	−1.161
CS_2	C	−1.096	0.862	−0.234	−1.096	8.521	−4.948	2.477
	S	0.548	−0.431	0.117	0.548	−4.269	2.471	−1.250
HCCH	C	−0.121	−0.090	−0.211	−0.121	−0.932	0.823	−0.230
	H	0.121	0.090	0.211	0.121	0.929	−0.823	0.227
NCCN	C	0.836	−0.575	0.261	0.836	−3.463	2.440	−0.187
	N	−0.836	0.574	−0.262	−0.836	3.467	−2.434	0.197

elements (see Figure 4; $p_{xx}^{(O)}$, $p_{xx}^{(H)}$, $p_{zz}^{(O)}$, and $p_{zz}^{(H)}$ elements in Table 12). Dipole flux contributions are small for these elements. On the other hand, charge flux contributions are zero by symmetry for the out-of-plane tensor elements. Static-charge contributions predominate for these elements with partial cancellations from dipole fluxes, as can be seen in Table 12.

For all the methane tensor elements, the charge flux and dipole flux contributions are much larger than the contributions from the carbon and hydrogen atomic charges. Charge, charge flux, and dipole flux contributions are all important for the $\partial p_z/\partial z_A$ elements of the carbon and oxygen atoms of formaldehyde, whereas they are quite small for the hydrogen atom. These dipole-moment derivatives are parallel to the principal symmetry axis of formaldehyde. Charge contributions from carbon and oxygen are predominant for in-plane tensor elements perpendicular to the principal symmetry axis, $p_{xx}^{(A)}$, although the dipole flux contribution from the oxygen atom is almost as large in absolute value but opposite in sign to its charge contribution. The out-of-plane charge flux contributions are, of course, zero.

TABLE 12: AIM Charge (C), Charge Flux (CF), and Dipole Flux (DF) Contributions to Polar Tensor Elements of the Nonlinear Molecules Calculated at the MP2/6-311++G(3d,3p) Level (units of electrons, e)

		$p_{xx}^{(A)}$			
molecule	atom	C	CF	DF	total
H_2O	O	−1.159	0.812	−0.122	−0.469
	H	0.580	−0.410	0.061	0.231
H_2CO	C	1.048	−0.234	−0.064	0.750
	O	−1.040	−0.140	0.741	−0.439
	H	−0.004	0.192	−0.341	−0.153
CH_4	C	0.086	−0.492	0.390	−0.016
	H	−0.022	−0.087	0.156	0.048

		$p_{yy}^{(A)}$			
molecule	atom	C	CF	DF	total
H_2O	O	−1.159	0.000	0.451	−0.708
	H	0.580	0.000	−0.225	0.355
H_2CO	C	1.048	0.000	−0.917	0.131
	O	−1.040	0.000	0.719	−0.321
	H	−0.004	0.000	0.098	0.094
CH_4	C	0.086	−0.488	0.394	−0.008
	H	−0.022	−0.089	0.164	0.054

		$p_{zz}^{(A)}$			
molecule	atom	C	CF	DF	total
H_2O	O	−1.159	0.710	0.130	−0.319
	H	0.580	−0.355	−0.066	0.159
H_2CO	C	1.048	−1.574	1.432	0.906
	O	−1.040	1.449	−1.183	−0.774
	H	−0.004	0.060	−0.127	−0.071
CH_4	C	0.086	−0.483	0.394	−0.003
	H	−0.022	0.532	−0.614	−0.104

		$p_{xz}^{(A)}$		
molecule	atom	CF	DF	total
H_2O	H1	0.315	−0.224	0.091
H_2CO	H1	−0.210	0.283	0.073

		$p_{zx}^{(A)}$		
molecule	atom	CF	DF	total
H_2O	H1	0.258	−0.161	0.097
H_2CO	H1	−0.334	0.471	0.137

The charge and dipole flux contributions of both the oxygen and carbon atoms have opposite signs partially canceling one another. Electronic structure rearrangements for the molecular vibrations of H_2CO and CH_4 will be examined in future papers treating the X_2CY (X = F, Cl; Y = O, S) and $CX_{4-n}Y_n$ (X, Y = F, Cl, H, and n = 0, 1, ..., 4) families of molecules.

For almost all the polar tensor elements calculated in this work, the charge flux and dipole flux contributions cancel one another. The negative correlation between these two contributions can be clearly seen in the graph presented in Figure 5. As the charge flux contribution becomes more positive, the dipole flux one becomes more negative. A negative correlation coefficient of −0.97 shows that this relaxation effect is very strong. Investigation of other molecules should be undertaken to determine if this dipolar relaxation effect of electron density distortions owing to charge flux perturbations is a general phenomenon or not.

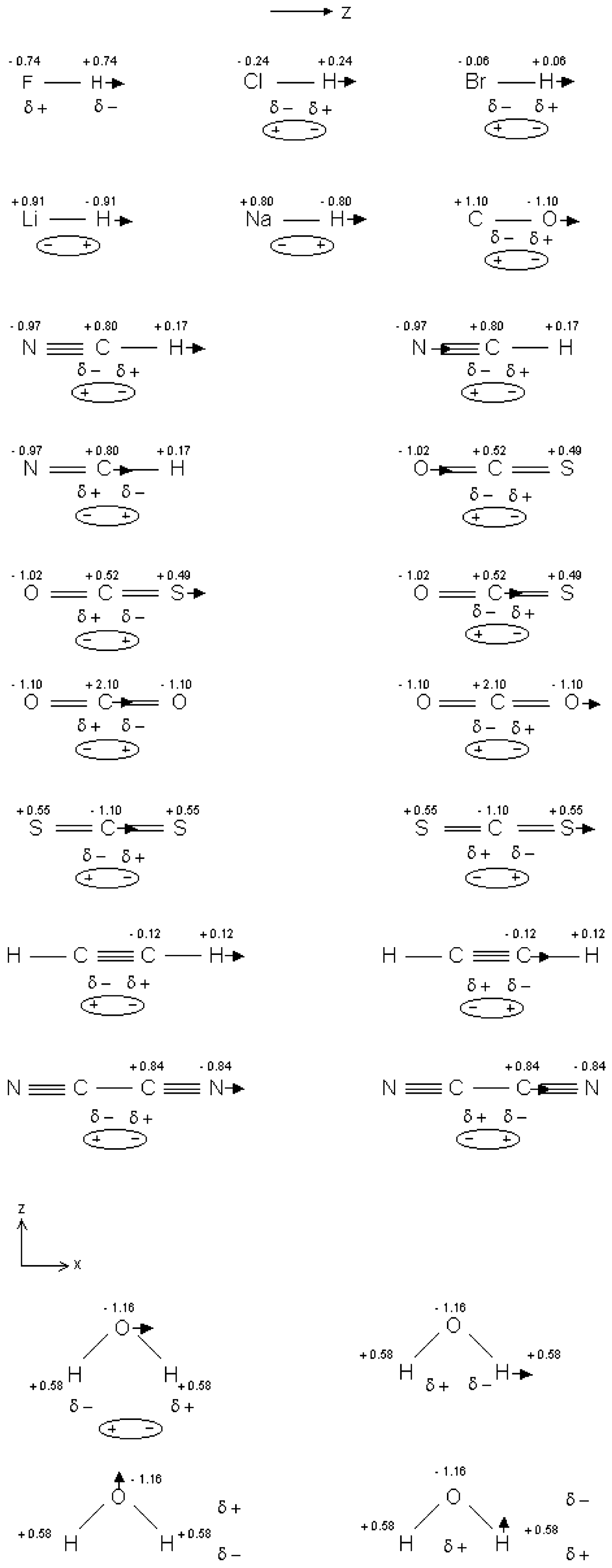

Figure 4. AIM charge, charge flux, and dipole flux contributions to polar tensor elements calculated at the MP2(FC)/6-311++G(3d,3p) level. Units of electrons. Atomic charges are indicated by signed numbers, charge flux by δ^+ and δ^-, and dipole fluxes by (− +) symbols. The arrows represent the atomic displacements.

Table 13 contains IR fundamental intensity sums for CO and the polyatomic molecules treated here. Experimental intensity sums[27,30] make up the first column, whereas the other two columns contain sums calculated directly from the MP2(FC)/6-311++G(3d,3p) approach and those obtained using the corresponding AIM parameters in the CCFDF model. The intensity sums calculated using the AIM parameters agree within 14.9 km mol^{-1} of the sums calculated directly from the molecular wave function. The largest discrepancy occurs for the water molecule, 33.9 km mol^{-1}. This is due to large

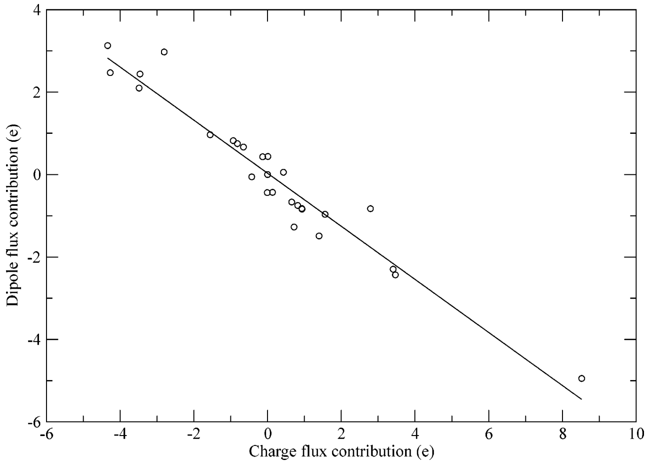

Figure 5. Charge flux vs dipole flux contributions to parallel polar tensor elements for the atoms of the linear molecules studied here.

TABLE 13: Experimental and Calculated IR Fundamental Intensity Sums (km mol^{-1}) for Polyatomic Molecules and CO[a]

	exp[b]	MP2	AIM
CO	61.2	35.9	36.9
HCN	111.0	149.0	156.3
OCS	611.1	677.3	679.0
CO_2	628.0	636.4	644.2
CS_2	555.0	600.5	604.1
HCCH	259.0	275.1	292.3
NCCN	41.4	52.3	52.3
H_2O	100.4[c]	145.0	111.1
H_2CO	264.7	261.3	252.1
CH_4	102.2	85.2	61.3

[a] Intensity sums were calculated directly from MP2(FC)/6-311++G(3d,3p) wave functions and the charge−charge flux−dipole flux model using AIM parameters. [b] Reference 30 except when indicated. [c] Reference 27.

contributions of the rotational correction to the IR intensity sum, Ω,

$$\sum_{i=1}^{3N-6} A_i = K\sum_{A}^{N}\sum_{\alpha}\sum_{\beta}\frac{1}{M_A}\left(\frac{\partial p_\alpha}{\partial \beta_A}\right)^2 - \Omega \tag{6}$$

where α and β are equal to x, y, and z and M_A is the mass of atom A. Now, Ω is a sum of terms containing the squares of dipole-moment components divided by the moments of inertia. As already pointed out, the AIM dipole moment of water has one of the largest deviations in Table 2 when compared to moments calculated directly from the molecular wave function. This is especially critical for determining the intensity sum, because the rotational contribution is unusually large for the water molecule, more than 350 km mol^{-1}.

4. Forces between a Charged Particle and a Molecule

Electrostatic forces between charged particles and molecules described by AIM quantities can also be calculated. The interaction energy of a system containing a molecule and a positively charged particle is given by

$$U = \sum_i q_i V_i - \sum_i m_i \cdot E_i + ... \tag{7}$$

where the first sum represents the contribution of the atomic charges and the second is the atomic dipole participation. V_i and E_i are, respectively, the external electric potential and field at the ith nucleus.

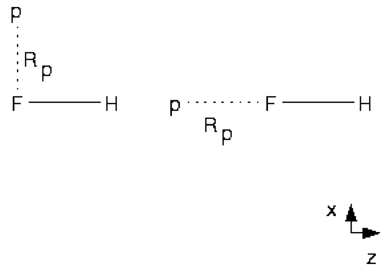

Figure 6. Molecular arrangements used for calculation of the forces between a charged particle (+0.1 e) and the HF molecule.

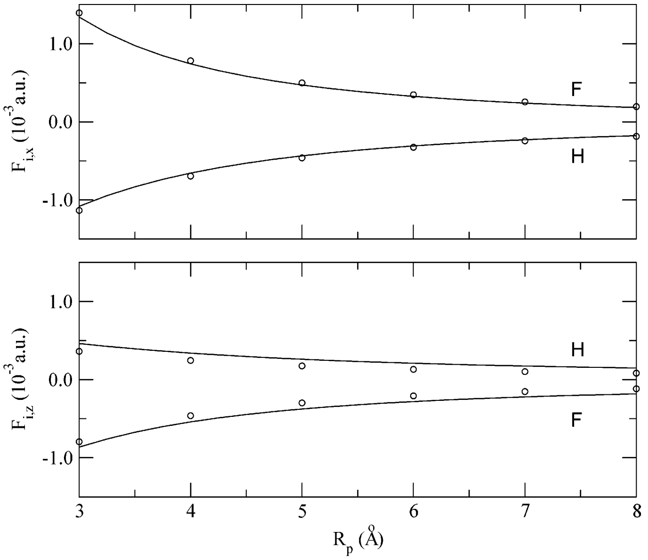

Figure 7. Forces exerted by a charged particle (+0.1 e) over the HF molecule.

These forces, after truncation to include only atomic charge and atomic dipole contributions, are represented by

$$F_{A,x} = -\partial U/\partial r_{A,x} = q_A E_A + \sum_i (\nabla_{A,x} q_i) V_i + m_A \cdot \nabla_{A,x} E_A - \sum (\nabla_{A,x} m_i) \cdot E_i \tag{8}$$

where the terms represent, from left to right, the partial charge, charge flux, atomic dipole, and atomic dipole flux contributions.[31] All these contributions have already been calculated and are in Tables 1 and 3−8. The magnitude chosen for the charged particle was +0.1 e to reduce the effects of polarizability.[31] The molecules studied were HF and CO. Perpendicular and collinear arrangements were studied, as shown in Figure 6. The molecular arrangement for CO was similar to that employed for HF with the carbon and oxygen atoms, respectively, at the F and H positions in Figure 6. The distance range between the charged particle and the molecule (R_p) was 3−8 Å.

Figure 7 shows the forces for the HF molecule. The lines represent the forces calculated directly from the molecular wave function obtained with the MP2(FC)/6-311++G(3d,3p) approach, and the open circles represent values calculated with eq 8 and AIM quantities.

The perpendicular forces are very well reproduced by the AIM quantities. In this arrangement, only the atomic charges and atomic dipole fluxes show significant participation. The atomic dipole contributions are insignificant, because the scalar product of eq 8 is zero for fluorine and very small for hydrogen.

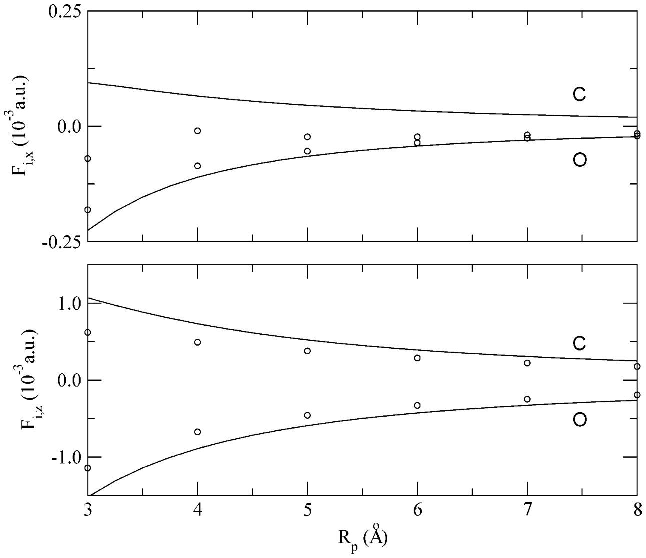

Figure 8. Forces exerted by a charged particle (+0.1 e) over the CO molecule.

The charge flux for a perpendicular atomic displacement is zero for linear systems.

On the other hand, the agreement between the MP2(FC)/6-311++G(3d,3p) collinear forces and the AIM derived values for HF is not quite as good. However, the participation of terms eliminated by truncation of the multipolar expansion to the atomic dipoles may be much more important in this case. Even so, the agreement is still satisfactory.

Figure 8 presents the CO case. The first thing to be noted is that the perpendicular forces for this molecule are very small, as can be seen by the scale change. However, the atomic charges for this molecule are very high (1.1 e), even higher than those for HF. Hence, the fact that perpendicular forces are almost negligible points to the conclusion that the other terms, such as the atomic dipole flux, must act in a contrary direction, almost canceling the charge contribution. Moreover, higher-order terms for eq 8 must be taken into account in order to correctly predict the perpendicular forces for CO. On the other hand, collinear forces for this molecule are reproduced by AIM quantities with a similar quality to those for HF.

5. Conclusions

AIM formalism is an important tool to study molecular electronic distributions. It is able to reproduce the molecular dipole moment as well as its derivatives, determining GAPT charges and providing an accurate classical model for understanding IR fundamental intensities.

The importance of considering atomic dipoles in addition to atomic charges in models to calculate dipole-moment derivatives and IR intensity sums is clearly demonstrated here. Furthermore, atomic charges alone are not able to account for the anisotropic behavior of the force between charged particles and molecules in different arrangements, such as the perpendicular and collinear ones investigated here.

It is encouraging to know that dipole-moment derivatives and IR intensity sums can be accurately calculated without including quadrupole and higher ordered terms in the model. The dipole-moment derivatives have been shown to be closely related to nuclear electric shielding tensors by Lazzeretti and co-workers.[34] These tensors are sensitive measures of electron densities close to nuclei in molecules and are proportional to the forces acting on nuclei when a molecule is placed in an external electric field. As such, one can expect to be able to calculate these tensors and forces from atomic charges and dipoles.

Moreover, AIM atomic multipoles can predict the forces between charged particles and molecules, as illustrated by the HF and CO examples, which is a rare characteristic of this kind of atomic model. The model proposed by Dinur and co-workers can also reproduce these forces for planar molecules.[32,33] As such, one can expect that atomic dipoles are important for molecular dynamics simulations as well as for interpreting chemical reactivities.

Acknowledgment. The authors are grateful to FAPESP and CNPq for partial financial support. R.L.A.H. also thanks FAPESP for doctoral fellowship.

References and Notes

(1) Dinur, U. *Chem. Phys. Lett.* **1990**, *166*, 211.
(2) Qian, W.; Krimm, S. *J. Phys. Chem. A* **1996**, *100*, 14602.
(3) Qian, W.; Krimm, S. *J. Phys. Chem. A* **1997**, *101*, 5825.
(4) Qian, W.; Krimm, S. *J. Phys. Chem. A* **2001**, *105*, 5046.
(5) Palmo, K.; Krimm, S. *J. Comput. Chem.* **1998**, *19*, 754.
(6) King, W. T.; Mast, G. B. *J. Phys. Chem.* **1976**, *80*, 2521.
(7) Ferreira, M. M. C. *J. Phys. Chem.* **1990**, *94*, 3220.
(8) Choi, C. H.; Kertesz, M. *Chem. Phys. Lett.* **1996**, *263*, 697.
(9) Mulliken, R. S. *J. Chem. Phys.* **1955**, *23*, 1833; *J. Chem. Phys.* **1955**, *23*, 1841.
(10) Mulliken, R. S. *J. Chem. Phys.* **1962**, *36*, 3428.
(11) Cioslowski, J. *J. Am. Chem. Soc.* **1989**, *111*, 8333.
(12) Bader, R. F. W. *Atoms in Molecules: a Quantum Theory*; Clarendon Press: Oxford, 1990.
(13) Bader, R. F. W. *Acc. Chem. Res.* **1985**, *18*, 9.
(14) Bader, R. F. W.; Larouche, A.; Gatti, C.; Carrol, M. T.; MacDougall, P. J.; Wiberg, K. B. *J. Chem. Phys.* **1987**, *87*, 1142.
(15) Wiberg, K. B.; Rablen, P. R. *J. Comput. Chem.* **1993**, *12*, 1504.
(16) Haiduke, R. L. A.; de Oliveira, A. E.; Bruns, R. E. *J. Phys. Chem. A* **2004**, *108*, 6788.
(17) Frisch, M. J.; Trucks, G. W.; Schlegel, H. B.; Scuseria, G. E.; Robb, M. A.; Cheeseman, J. R.; Zakrzewski, V. G.; Montgomery, J. A., Jr.; Stratmann, R. E.; Burant, J. C.; Dapprich, S.; Millam, J. M.; Daniels, A. D.; Kudin, K. N.; Strain, M. C.; Farkas, O.; Tomasi, J.; Barone, V.; Cossi, M.; Cammi, R.; Mennucci, B.; Pomelli, C.; Adamo, C.; Clifford, S.; Ochterski, J.; Petersson, G. A.; Ayala, P. Y.; Cui, Q.; Morokuma, K.; Malick, D. K.; Rabuck, A. D.; Raghavachari, K.; Foresman, J. B.; Cioslowski, J.; Ortiz, J. V.; Stefanov, B. B.; Liu, G.; Liashenko, A.; Piskorz, P.; Komaromi, I.; Gomperts, R.; Martin, R. L.; Fox, D. J.; Keith, T.; Al-Laham, M. A.; Peng, C. Y.; Nanayakkara, A.; Gonzalez, C.; Challacombe, M.; Gill, P. M. W.; Johnson, B. G.; Chen, W.; Wong, M. W.; Andres, J. L.; Head-Gordon, M.; Replogle, E. S.; Pople, J. A. *Gaussian 98*, revision A.7; Gaussian, Inc.: Pittsburgh, PA, 1998.
(18) Wiberg, K. G.; Hadad, C. M.; LePage, T. J.; Breneman, C. M.; Frisch, M. J. *J. Phys. Chem.* **1992**, *96*, 671.
(19) Lide, D. R., Ed. *CRC Handbook of Chemistry and Physics*, 78th ed.; CRC Press: Boca Raton, FL, 1997−1998.
(20) Bruns, R. E.; Brown, R. E. *J. Chem. Phys.* **1978**, *68*, 880.
(21) Kim, K.; King, W. T. *J. Chem. Phys.* **1979**, *71*, 1967.
(22) Person, W. B.; Brown, K. G.; Steele, D.; Peters, D. *J. Am. Chem. Soc.* **1981**, *85*, 1998.
(23) Jona, P.; Gussoni, M.; Zerbi, G. *J. Phys. Chem.* **1981**, *85*, 2210.
(24) Kim, K.; King, W. T. *J. Mol. Struct.* **1979**, *57*, 201.
(25) Smit, W. M. A.; Van Straten, A. J.; Visser, T. *J. Mol. Struct.* **1978**, *48*, 177.
(26) Kim, K.; King, W. T. *J. Chem. Phys.* **1984**, *80*, 974.
(27) Zilles, B. A.; Person, W. B. *J. Chem. Phys.* **1983**, *79*, 65.
(28) Castiglioni, C.; Gussoni, M.; Zerbi, G. *J. Chem. Phys.* **1985**, *82*, 3534.
(29) de Oliveira, A. E. Ph.D. Thesis, Universidade Estadual de Campinas, Campinas, 1999.
(30) de Oliveira, A. E.; Haiduke, R. L. A.; Bruns, R. E. *J. Phys. Chem. A* **2000**, *104*, 5320.
(31) Dinur, U. *J. Chem. Phys.* **1991**, *95*, 6201.
(32) Dinur, U.; Hagler, A. T. *J. Chem. Phys.* **1989**, *91*, 2949.
(33) Dinur, U.; Hagler, A. T. *J. Chem. Phys.* **1989**, *91*, 2959.
(34) Lazzeretti, P.; Zanasi, R. *J. Chem. Phys.* **1985**, *83*, 1218.